Rotational symmetry of the surface second-harmonic generation of zinc-blende-type crystals

Chikashi Yamada and Takahiro Kimura
Optoelectronics Technology Research Laboratory, 5-5 Tohkodai, Tsukuba, Ibaraki 300-26, Japan
(Received 30 August 1993; revised manuscript received 20 December 1993)

The symmetry properties of surface second-harmonic generation (SHG) have been studied for compound semiconductor materials, such as GaAs, in which the nonlinear susceptibility of the bulk does not vanish. The rotation-angle dependence (anisotropy) of the intensity of surface-reflection SHG for singular as well as vicinal surfaces, with and without surface tensor components, was examined and compared with the existing experimental results.

I. INTRODUCTION

Surface second-harmonic generation (SHG) has the potential to be a unique tool for studying surface phenomena. For surfaces of centrosymmetric materials, such as those of Si and metals, there has been a resurgence in studies of surface SHG within this decade or so,[1] after a rather long interval since the work of Bloembergen and co-workers.[2] This is because in these materials, having a center of symmetry, bulk SHG is forbidden (within the electric dipole approximation) and, therefore, SHG is inherently surface specific.

In compound semiconductors, on the other hand, a bulk contribution to SHG is present; to make things worse, it is well known that GaAs, for example, is one of the materials having large second-order susceptibilities. It is therefore necessary to establish a method by which the surface and bulk contributions can be separated, so that surface SHG can become a useful method for studying compound semiconductor surfaces. Chang and Bloembergen[3] have worked out the incident-angle dependence of the bulk contribution for various combinations of the azimuthal angle and polarization. Stehlin *et al.*[4] have elucidated possible combinations of the polarization of incident and second-harmonic light and crystal azimuths in which only the surface contribution can be deduced for typical low-index surfaces, i.e., (001), (110), and (111). Sipe, Moss, and Van Driel[5] have developed a theory of rotation-angle dependence of surface SHG from cubic centrosymmetric crystals. In this paper, we calculate the rotation-angle dependence of the surface SH intensity from noncentrosymmetric cubic crystals: for low-index surfaces as well as some vicinal surfaces, with and without surface specific susceptibilities.

More specifically, we wish to show that our preliminary results[6] cannot be explained without introducing surface tensor components, even if a possible misorientation of the crystal might exist: A different rotational anisotropy of the SH intensity distribution [C_S (in the point-group notation) $\equiv m$ (in the crystal-symmetry group notation) or lower] would be predicted for the miscut (vicinal) surfaces without a surface contribution. On the contrary, a C_{2v} ($\equiv mm2$) symmetry is expected for the case of a singular surface possessing surface-specific second-order susceptibility tensors. We would also like to show that by observing the rotation-angle dependence, small differences in the surface contributions are *magnified* by interference with the strong bulk component.

In this calculation we restrict ourselves to dipolar second-harmonic generation, because the higher-order (electric quadrupolar or magnetic dipolar) contributions are thought to be orders of magnitude smaller than the electric dipolar contribution.[7]

II. OUTLINE OF CALCULATION

A. Bulk contribution

It is well known that in crystals with a zinc-blende structure, such as GaAs, the bulk second-order susceptibility tensor has only one component,

$$\chi^{(2)}_{xyz}=\chi^{(2)}_{yzx}=\chi^{(2)}_{zxy}=\chi^{(2)}_{xzy}=\chi^{(2)}_{yxz}=\chi^{(2)}_{zyx} , \tag{1}$$

where x, y, and z correspond to the principal axes of the crystal.[2,8] The transformation law for $\chi^{(2)}$ corresponding to the rotation of the coordinate system is[8]

$$\chi^{(2)}_{\mu\alpha\beta}=\sum\sum\sum R_{\mu u}R_{\alpha a}R_{\beta b}\chi^{(2)}_{uab} , \tag{2}$$

where R is a 3×3 matrix representing the rotation of the coordinate system from (u,a,b) to (μ,α,β).

We define a new set of coordinates (x',y',z') and a rotation matrix (R) for a certain crystal-face orientation, such that the z' axis is perpendicular to the crystal face,

$$\begin{bmatrix}x'\\y'\\z'\end{bmatrix}=R\begin{bmatrix}x\\y\\z\end{bmatrix} , \tag{3}$$

where (x,y,z) represents the principal-axis system of the crystal ([100], [010], [001]). In Fig. 1 we show the coordinate system.

A new set of coordinates for the (110) singular face, for example, is obtained by applying the following transformation:

$$R_1=\begin{bmatrix}-1/\sqrt{2} & 1/\sqrt{2} & 0\\ 0 & 0 & 1\\ 1/\sqrt{2} & 1/\sqrt{2} & 0\end{bmatrix} . \tag{4}$$

For a vicinal (001) face tilted by an angle δ towards the direction of an angle ψ from the [100] axis (x axis), the rotation matrix can be expressed by

$$R=\begin{bmatrix} \cos^2\psi\cos\delta+\sin^2\psi & \sin(2\psi)\sin^2(\delta/2) & \cos\psi\sin\delta \\ \sin(2\psi)\sin^2(\delta/2) & \cos^2\psi+\cos^2\psi\cos\delta & -\sin\psi\sin\delta \\ -\cos\psi\sin\delta & \sin\psi\sin\delta & \cos\delta \end{bmatrix} . \quad (5)$$

Following Sipe, Moss, and van Driel,[5] we define a set of unit vectors for the incident light beam s, k, and z such that s and k lie on the crystal face, perpendicular and parallel to the plane of incidence, respectively, and $z=z'$ is the surface normal,

$$\begin{bmatrix} s \\ k \\ z \end{bmatrix} = R_0 \begin{bmatrix} x' \\ y' \\ z' \end{bmatrix} = \begin{bmatrix} \sin\varphi & -\cos\varphi & 0 \\ \cos\varphi & \sin\varphi & 0 \\ 0 & 0 & 1 \end{bmatrix} \begin{bmatrix} x' \\ y' \\ z' \end{bmatrix} . \quad (6)$$

Here φ is the angle between k and x', the azimuthal angle. By multiplying all of the relevant matrices, e.g., for the (110) face $R=R_0R_1$, and using Eq. (2), we obtain χ tensor elements in the beam coordinate system (s,k,z). This new tensor describes the second-harmonic polarization for an arbitrary face of the crystal by the incident laser light with an azimuthal angle of φ,

$$P_i^{(2\omega)}(\varphi)=\sum\sum\chi^{(2)}_{ilm}(\varphi)E_l^{(\omega)}E_m^{(\omega)} , \quad (7)$$

where i, l, and m run through s, k, and z. Here, we mention that for a vicinal surface the rotation of the crystal is assumed to be around the surface normal, not around the original singular axis, although the latter choice is adopted in some experiments.[9,10]

The components of the fundamental field in the medium are resolved into the following s- and p-polarized fields:

$$E_S=E_{0s}t_s,\quad E_k=f_cE_{0p}t_p\ ,E_z=f_sE_{0p}t_p\ , \quad (8)$$

where t_s and t_p are the Fresnel coefficients and f_c and f_s are defined so that if n (index of refraction) were real, f_c and f_s would simply be the cosine and sine of the angle of refraction.[5]

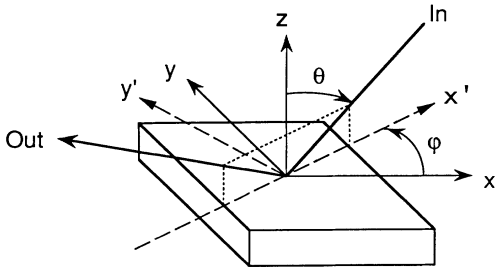

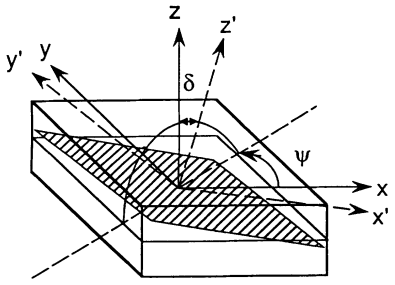

FIG. 1. Definition of the rotation angle for the singular (001) face (upper figure) and the vicinal face (lower figure).

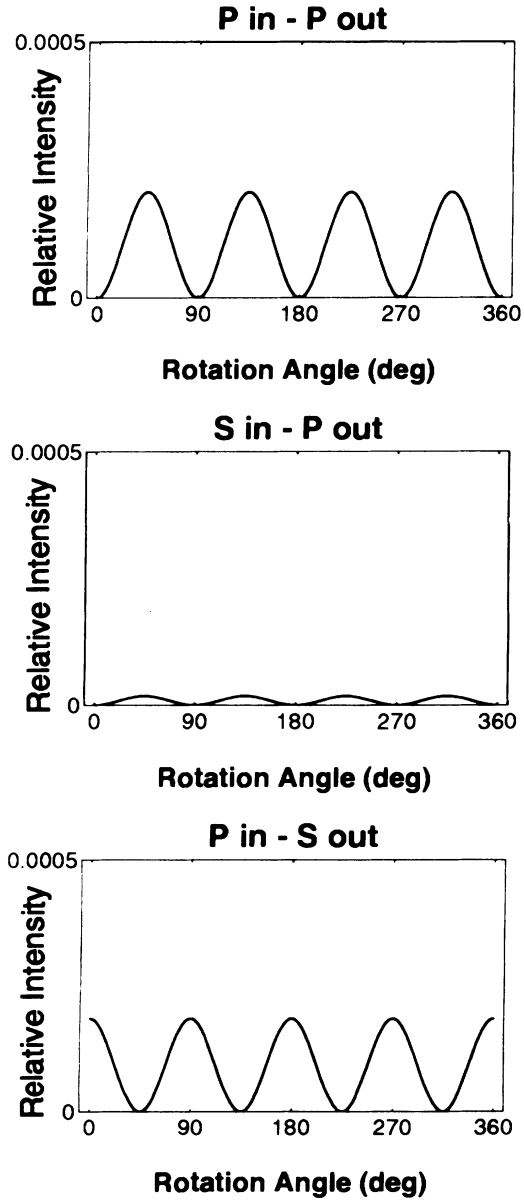

FIG. 2. Rotation-angle dependence of the surface SHG from the (001) face of a GaAs crystal. The incident angle is 60° and the wavelength of the input light is 532 nm. Only the bulk susceptibility is considered.

Similarly, the second-harmonic fields generated by polarization of the form of (7) are decomposed into s- and p-polarized components,

$$E_s^{(2\omega)} = A_s \Omega L_{\text{eff}} P_s^{(2\omega)}$$

and

$$E_p^{(2\omega)} = A_p \Omega L_{\text{eff}} [F_s P_z^{(2\omega)} - F_c P_k^{(2\omega)}] , \tag{9}$$

where $\Omega = 2\omega/c$ is the magnitude of the wave vector (in free space) of the second-harmonic light, $L_{\text{eff}} = (W + 2w)^{-1}$ is the effective phase-matching distance[4] with W and w represent the z component of the wave vectors of the second harmonic and fundamental light, respectively, in the crystal.

The proportionality constants, A_s and A_p (given in Ref. 5), are independent of the angle of rotation, but are dependent on the incident angle and optical frequency through a change in the index of refraction. The coefficients F_S and F_c are defined similarly to f_s and f_c for the second-harmonic field. The SH intensity is proportional to the absolute square of $E^{(2\omega)}$.

B. Surface contribution

For surfaces possessing a certain symmetry, only a few tensor elements remain nonzero. These surface second-order susceptibility tensor elements have already been tabulated.[8,11] It must be noted that, in general, the symmetry axes are not coincident with the principal axes of the bulk crystal. For example, the singular (001) face has two mirror planes perpendicular to each other in the directions of [110] and [1$\bar{1}$0], which are 45° off from the x ([100]) and y ([010]) axes. The same is true even if the surface is reconstructed, e.g., 2×4, 4×2, etc. We call the intersections of the mirror planes with the crystal face ξ and η.

We use the symbol ∂ to denote the surface (dipolar) second-order susceptibilities, and Π for surface polarization, e.g.,

$$\Pi_\xi = \partial_{\xi\eta z} E_\eta E_z, \quad \text{etc.}, \tag{10}$$

in the (ξ,η,z) system.

In a particular case of the (001) face, a rotation matrix of the form

$$\begin{bmatrix} 1/\sqrt{2} & -1/\sqrt{2} & 0 \\ 1/\sqrt{2} & 1/\sqrt{2} & 0 \\ 0 & 0 & 1 \end{bmatrix} \tag{11}$$

must be applied to the Π's in order to obtain the polarization vector in the $(x',y',z') = (x,y,z)$ system. Further, the rotation matrix, R_0 [Eq. (6)], is multiplied to obtain the polarization vector in the (s,k,z) system. The second-harmonic field induced by the sheet of polarization can be written as[5]

$$E_{s,\text{surf}}^{(2\omega)} = A_s \Omega \Pi_s^{(2\omega)}$$

and (12)

$$E_{p,\text{surf}}^{(2\omega)} = A_p \Omega [F_s \varepsilon(2\omega)] \Pi_z^{(2\omega)} - F_c \Pi_k^{(2\omega)}] ,$$

where $\varepsilon(2\omega)$ is the dielectric constant at frequency 2ω. Here, we dropped the symbol i, which may be included in the ∂'s.

TABLE I. Symmetry of surface-reflection SHG from the (001) face.

Surface symmetry	Tensor elements[a] xyz (bulk only)	Rotational symmetry[b] $P_{\text{in}} - P_{\text{out}}$ 4	$S_{\text{in}} - P_{\text{out}}$ 4	$P_{\text{in}} - S_{\text{out}}$ 4	$S_{\text{in}} - S_{\text{out}}$ i.a.
C_{4v}	$z\xi\xi = z\eta\eta$	$mm2$	$mm2$	4	i.a.
(4)	$zzz, \xi\xi z = \eta\eta z$	$mm2$	4	4	i.a.
C_{2v}[c]	$z\xi\xi + z\eta\eta$	$mm2$	$mm2$	4	i.a.
($mm2$)	$\xi\xi z + \eta\eta z$	$mm2$	4	4	i.a.
	$z\xi\xi - z\eta\eta$, $\xi\xi z - \eta\eta z$	4	4	4	i.a.
C_s	$\xi\xi\xi, \xi\eta\eta$	$m\perp\eta$	$m\perp\eta$	$m\perp\eta$	$mm2$
($m\perp\eta$)	ξzz	$m\perp\eta$	4	$m\perp\eta$	i.a.
	$zz\xi$	$m\perp\eta$	4	4	i.a.
C_1	$\eta\xi\xi, \xi\xi\eta$, $\eta\xi\eta, \eta\eta\eta$	$m\perp\xi$	$m\perp\xi$	$m\perp\xi$	$mm2$
	ηzz	$m\perp\xi$	4	$m\perp\xi$	i.a.
	$\xi\eta z, \eta\xi z$	4	4	$mm2$	i.a.
	$z\xi\eta$	4	4	4	i.a.

[a]Only the suffixes are shown. The tensor elements are invariant under a permutation of the last two suffixes.

[b]From C_{4v} below, the resultant symmetry which is obtained by the interference of the bulk plus surface contributions is presented. The entry i.a. means inactive.

[c]If $\partial_{z\xi\xi} + \partial_{z\eta\eta} = 0$ and $\partial_{\xi\xi z} + \partial_{\eta\eta z} = 0$, fourfold symmetry is obtained. Individual terms, e.g., $\partial_{z\xi\xi}$ cause overall $mm2$ symmetry, but also changes the fourfold symmetric "component."

III. RESULTS

In the following calculation, we assume the bulk susceptibility to be unity, and only the relative magnitude of the surface susceptibilities with respect to the bulk susceptibility is taken into account.

Before proceeding to the results, we mention that, according to Koopmans, van der Woude, and Sawatzky,[12] we may observe at most the sixfold symmetry in the intensity distribution of SHG, since we take into account only the dipolar ($L=1$) second-harmonic ($M=2$) polarizations; then, $M+L=3$ gives the maximum symmetry number for the polarization and, therefore, the intensity (proportional to the square of the polarization) exhibits a 3×2 or sixfold symmetry. However, it must be noted that, in some cases, even if the surface symmetry is lower than n-fold, the SH intensity would exhibit a full $2n$-fold symmetry, depending on which surface tensor element is nonzero.[13] On the contrary, when the observed rotational symmetry of the SHG is low, the tensor elements which would have given a higher symmetry cannot be addressed without resorting to the absolute intensity.

We would also like to mention that in optically flat faces, even in a nominally singular surfaces, for example, there exist many local microscopic structures, as have recently been observed by scanning tunneling microscopy.[14,15] In such cases, the microscopic symmetry of the structures, such as monoatomic steps, etc. would allow some specific tensor element to exist. If the domains consisting of these structures are smaller than the spot size of the laser radiation, there would be a "superposition" of the symmetries. That is, we may observe a lower symmetry than expected if the newly introduced tensor is of different symmetry.

A. (001) face

Figure 2 shows the rotation-angle dependence of the SH intensity for a singular (001) face with only the bulk susceptibility χ_{xyz}. For three configurations ($P_{in}-P_{out}$, $S_{in}-P_{out}$, and $P_{in}-S_{out}$) the SH intensity distribution shows a C_{4v} symmetry, while for $S_{in}-S_{out}$ the SHG is

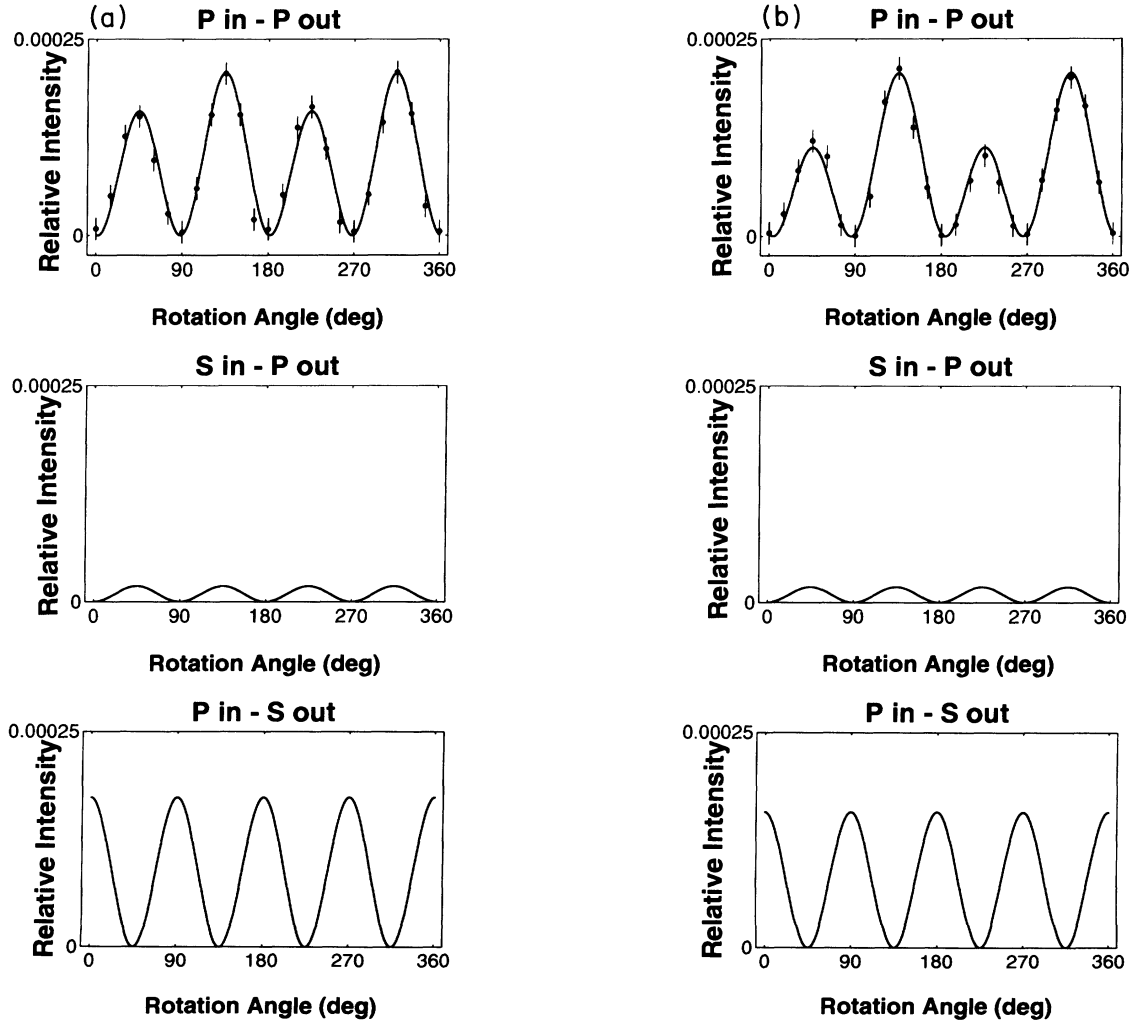

FIG. 3. Rotation-angle dependence of surface SHG with surface susceptibility of $\partial_{\xi\xi z}=-0.024$ (a) and $\partial_{\xi\xi z}=-0.04$ (b), corresponding to 2×1 and 4×6 reconstructions, respectively. The points with error bars are the observed SH intensity for the $P_{in}-P_{out}$ case of Ref. 6, normalized at the largest peaks. The angle of incidence is 60° and the wavelength of the input light is 580 nm.

forbidden.

Table I summarizes the results in cases where surface susceptibility is present. In Table I, the symmetry for each polarization condition is classified according to the ∂ tensor elements, which are allowed in each surface symmetry. Here, we mention that we cannot specify a certain surface tensor element as being responsible for causing anisotropy, even if the surface symmetry is known, i.e., there are always plural tensor elements which cause the same rotational symmetry. Therefore, the determination of the relevant tensor element(s) must rely upon other sources of information, e.g., the microscopic surface structure, which may be obtained either experimentally or theoretically.

The present authors have observed the rotational anisotropy on the (001) surface of GaAs.[6] They observed a twofold symmetry only for the $P_{\text{in}}-P_{\text{out}}$ case, and a fourfold symmetry for the $S_{\text{in}}-P_{\text{out}}$ case. Therefore, the relevant surface ∂ tensor is likely to be ∂_{zzz}, $\partial_{\xi\xi z}$, or $\partial_{\eta\eta z}$, or any combination of them (see Table I). They found that the amount of this anisotropy changes with the surface reconstruction.

To illustrate the advantage of observing the rotation-angle dependence, we plot in Fig. 3 the cases with a surface tensor elements of $\partial_{\xi\xi z}=-0.024$ [Fig. 3(a)] and $\partial\xi\xi z=-0.04$ [Fig. 3(b)], which closely simulate the observed rotational anisotropy of the 2×1 and 4×6 reconstructed surfaces in Ref. 6, respectively. In Fig. 3, $P_{\text{in}}-P_{\text{out}}$ case, the surface-specific SHG is represented at angles of 0°, 90°, 180°, and 270°, and is very small. However, the anisotropy, i.e., the intensity difference of the strong and weak peaks, which is the result of interference of bulk SHG with surface SHG, is quite discernible. The curve for the 4×6 reconstructed surface [Fig. 3(b)] is numerically represented by

$$|\alpha+\beta\sin(2\varphi)|^2 , \tag{13}$$

with $\alpha=-0.0023+0.0015i$ and $\beta=0.0142-0.0095i$.[16] Therefore, the anisotropy $[4\,\mathrm{Re}(\alpha)\mathrm{Re}(\beta)+4\,\mathrm{Im}(\alpha)\mathrm{Im}(\beta)=1.84\times10^{-4}]$ is about 25 times larger than the surface-specific component ($|\alpha|^2=7.29\times10^{-6}$), allowing one to easily observe the surface effect. The relative intensities of the large and small peaks are also reproduced by using ∂_{zzz} (0.035 for the 4×6 surface and 0.021 and the 2×1 surface) or $\partial_{\eta\eta z}$ (-0.06 for the 4×6 and -0.036 for the 2×1 surface), although the relative intensities between 2×1 and 4×6 differ from the experiment. Although the tensor elements $\partial_{z\xi\xi}$ or $\partial_{z\eta\eta}$ also give the same pattern for the $P_{\text{in}}-P_{\text{out}}$ case, the symmetry for $S_{\text{in}}-P_{\text{out}}$ is different from that found in the experiment in that they give a C_{2v} ($mm2$) symmetry instead of a $C_4(4)$ symmetry (see Table I).

Armstrong and co-workers[19–21] have reported the rotational anisotropy for the case of a *vicinal* (001) face of GaAs. Figure 4 shows the case of a vicinal (001) surface tilted toward the [110] direction by 2° (which is the vicinal angle of Ref. 18), where the surface contribution is assumed to be absent. For all combinations of the polarization of input and output beams, we have a mirror symmetry ($C_s=m$). A large anisotropy is obtained, especially for the $P_{\text{in}}-P_{\text{out}}$ case. The difference in the heights of

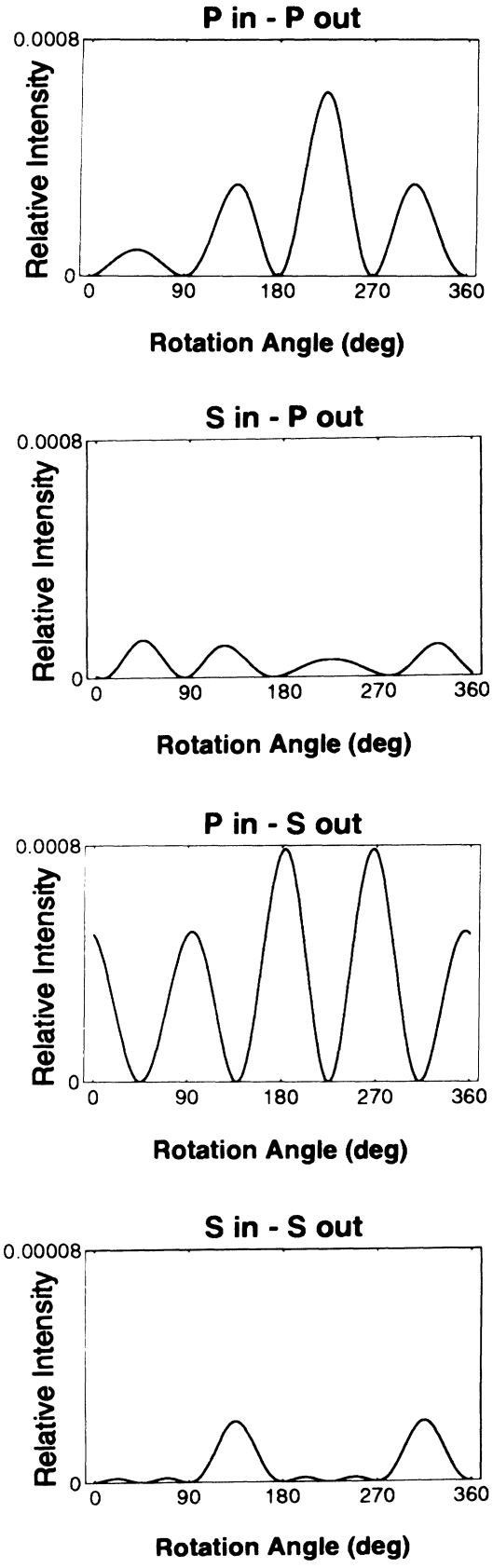

FIG. 4. Rotation-angle dependence of SHG from a vicinal (001) face tilted toward [110] by 2°. Only the bulk susceptibility is included. The angle of incidence is 45° and the wavelength of the input light is 1.06 μm.

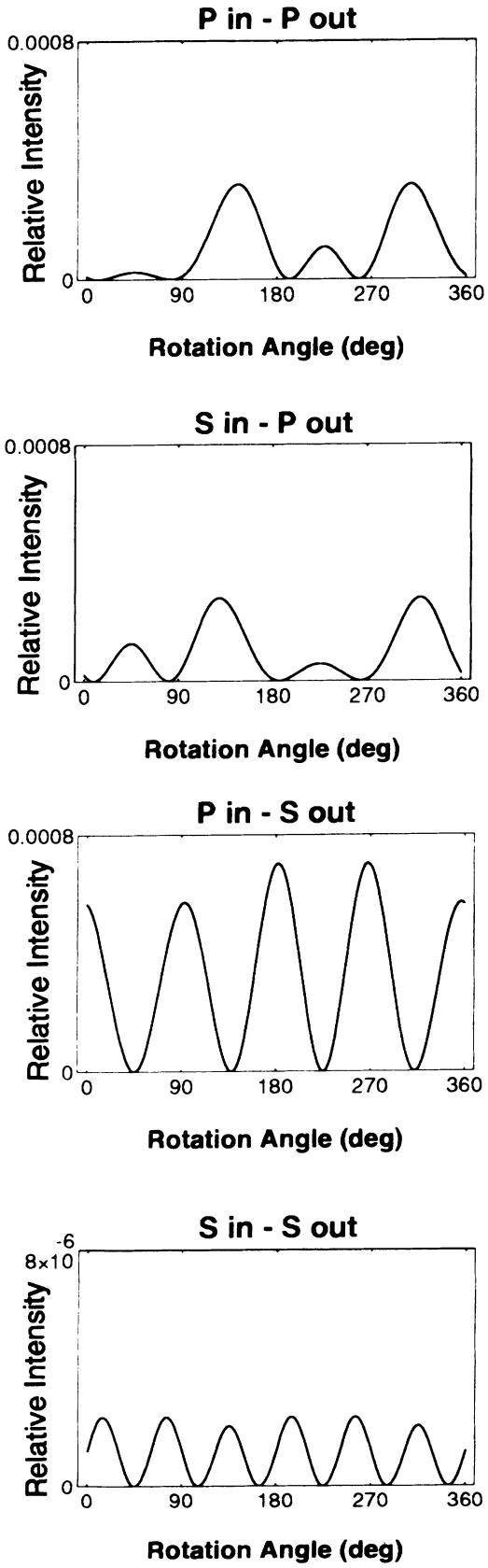

FIG. 5. Rotation-angle dependence of SHG from the vicinal (001) face. Surface tensor elements, $\partial_{z\xi\xi}=0.006$ and $\partial_{\xi\xi\xi}=0.01$, are included. The angle of incidence is 45° and the wavelength of the input light is 1.06 μm.

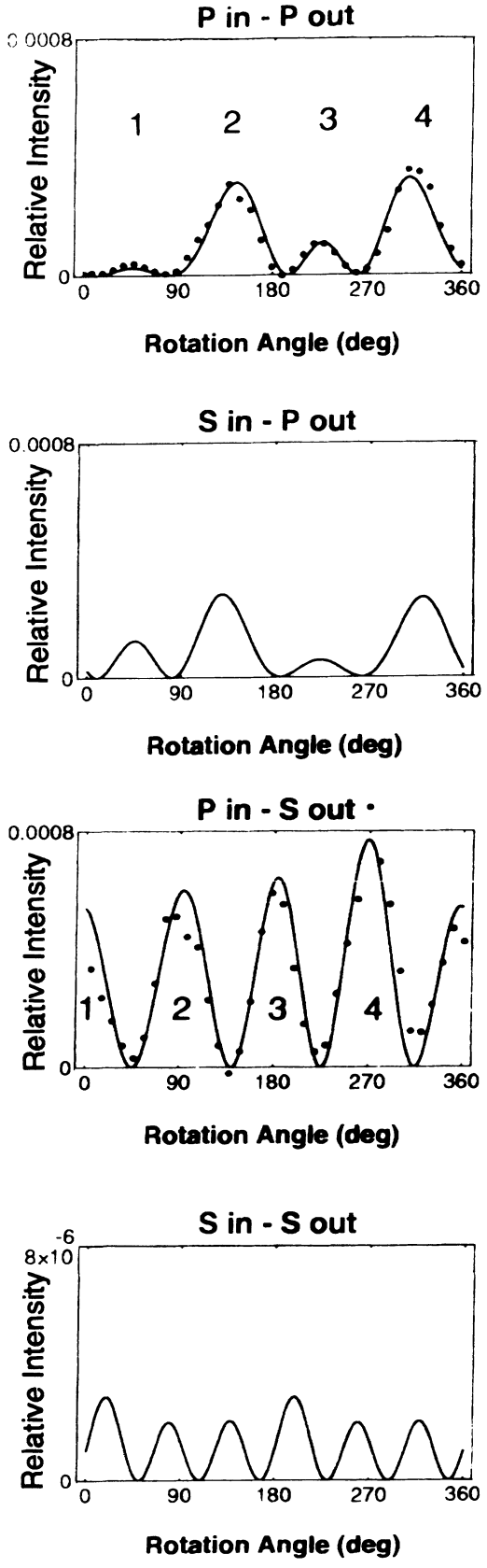

FIG. 6. Same as Fig. 5, with the direction of the tilt offset by 5° and $\partial_{\xi\eta z}=0.02$ was added. Also shown by closed circles are the experimental data of Ref. 20. In plotting the experimental points, a constant value was subtracted to match the zero level.

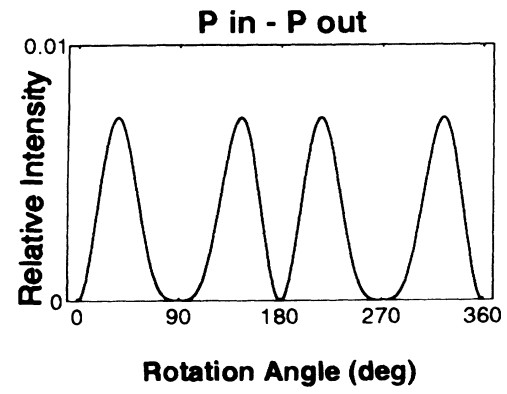

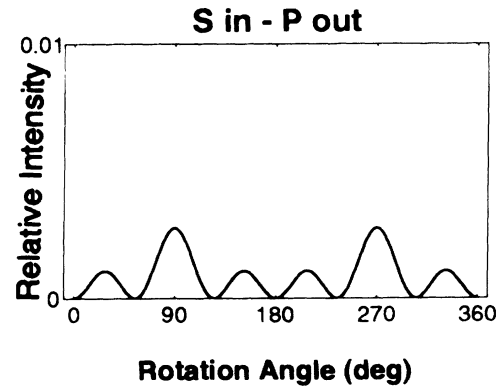

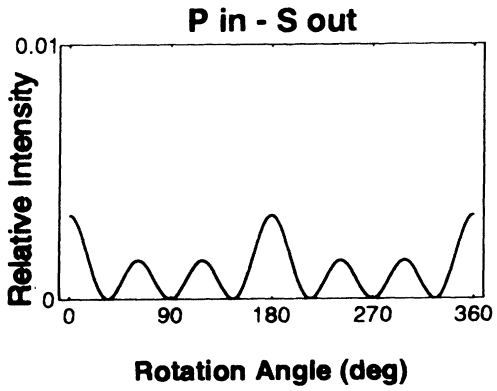

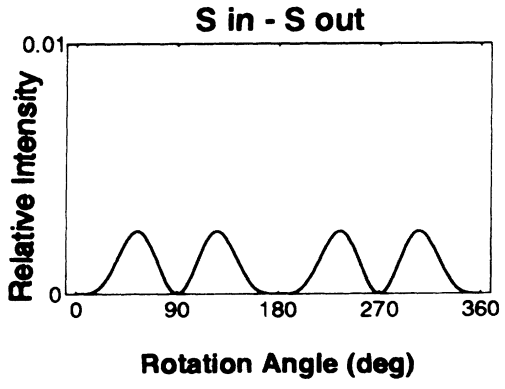

FIG. 7. Rotation-angle dependence of surface SHG from the (110) face. Only the bulk contribution is included. The angle of incidence is 45° and the wavelength of incident light is 1.06 μm.

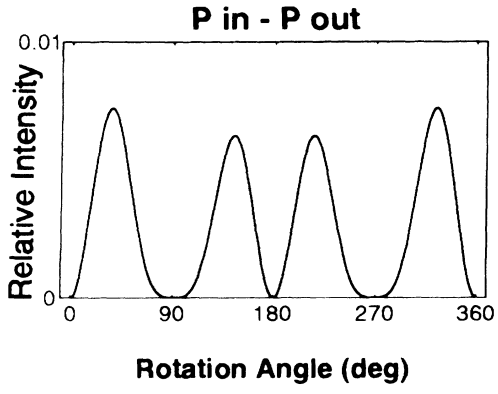

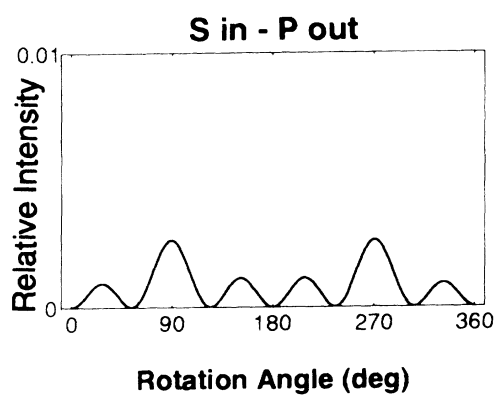

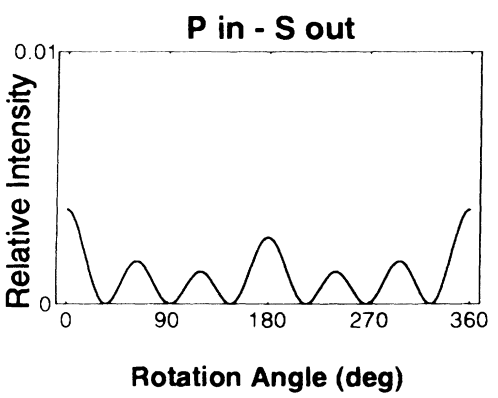

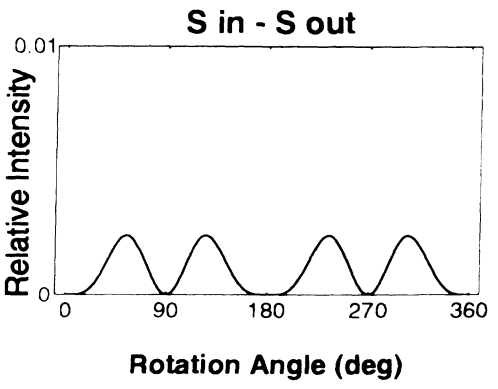

FIG. 8. Rotation-angle dependence of the surface SHG from a *vicinal* (110) face. Only the bulk contribution is considered. The angle of incidence is 45° and the wavelength of incident light is 1.06 μm.

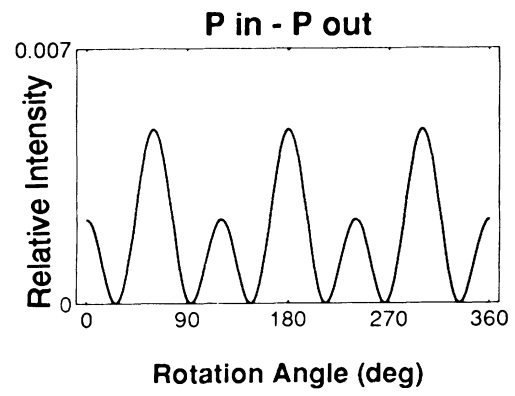

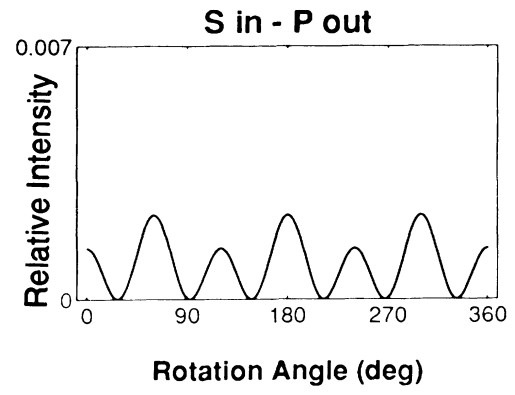

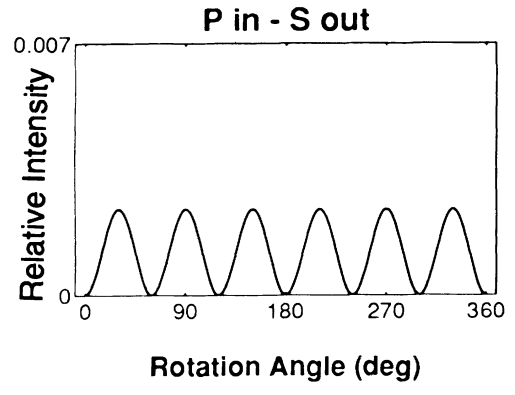

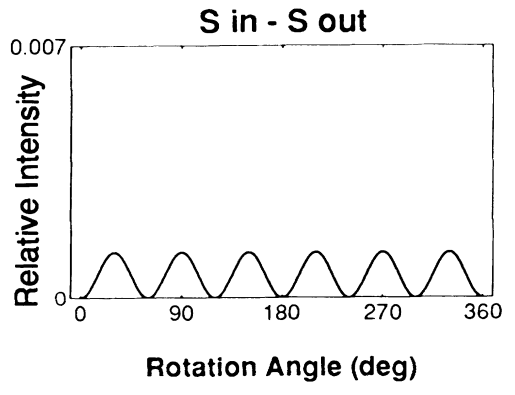

FIG. 9. Rotation-angle dependence of the surface SHG from the (111) face. The angle of incidence is 45° and the wavelength of incident light is 1.06 μm.

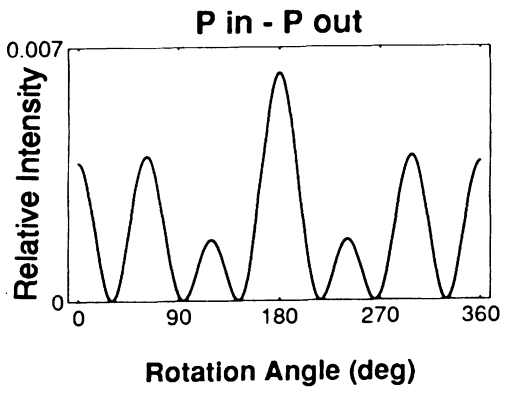

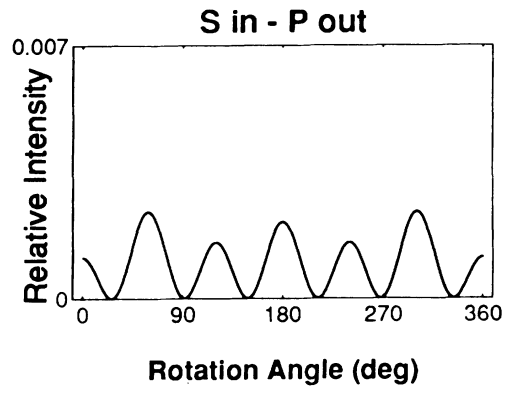

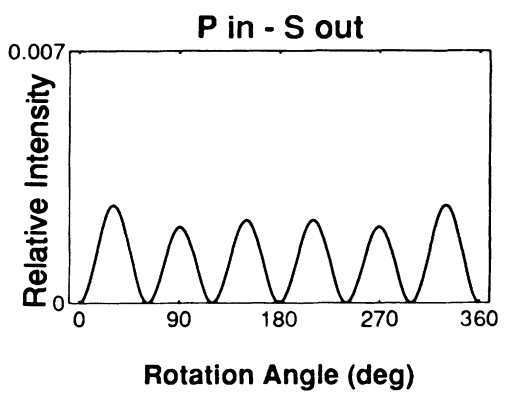

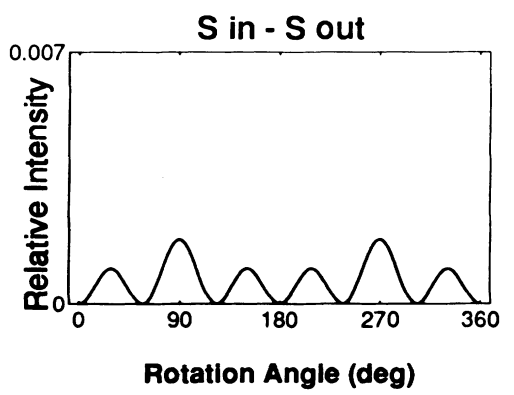

FIG. 10. Rotation-angle dependence of the surface SHG from a *vicinal* (111) face. The angle of incidence is 45° and the wavelength of incident light is 1.06 μm.

the largest and smallest peaks amounts to 70% of the sum of the two. We also notice that $S_{in}-S_{out}$ became allowed, although the intensity is very small (note the magnification of the figure). When the tilt is in other directions than [100] or [110], even the mirror symmetry would be lost.

Here in Fig. 4, we number the peaks from left to right as 1, 2, 3, and 4. By a comparison of this figure with the experimental plot (see Ref. 21 as well as Figs. 5 and 6), we find that in the $P_{in}-P_{out}$ case, (a) peaks 1 and 3 are too large compared with peaks 2 and 4; (b) the relative intensity of peaks 1 and 3 is different (peak 3 is too large). These mismatches are fixed by introducing, for example, (a) $\partial_{z\xi\xi}$ ($\partial_{z\eta\eta}$, ∂_{zzz}, or $\partial_{\xi\xi z}$ also give the same result) and (b) $\partial_{\xi\xi\xi}$ (or $\partial_{\xi zz}$, $\partial_{\xi\xi z}$, $\partial_{\xi\eta\eta}$) (see Table I). Figure 5 shows the "best fit" to the experimental result, in which $\partial_{z\xi\xi}=0.006$ and $\partial_{\xi\xi\xi}=0.01$ were used. The apparent difference in the intensity of peaks 2 and 4 of Ref. 21 cannot be explained as long as the mirror symmetry ($m\perp\eta$) is present. Since the same is true for the $P_{in}-S_{out}$ case, peaks 3 and 4 must have the same intensity. These discrepancies may be explained by either a nonideal cut of the crystal (the direction of the tilt), the domain formation with different symmetry axis, or possibly other experimental artifacts, e.g., polarization due to the window materials. For example, if we set the direction of the tilt to be off from [110] by 5°, i.e., $\psi=50°$, not 45°, the calculated rotation-angle dependence gives a closer *fit* to the experimental result, as shown in Fig. 6. In this calculation, another tensor element of $\partial_{\xi\eta z}=0.02$ (which is allowed only in C_1 symmetry) was also added to improve the fit for the $P_{in}-S_{out}$ case. In the present framework of the theory, there must be four zeros in the rotation-angle dependence of the SH signal as long as the surface component does not exceed the bulk contribution. In the fitting, therefore, we subtracted a constant from each data point, so that the data points with smallest intensity be shifted to zero. The surface tensor element $\partial_{\xi\xi\xi}$, $\partial_{\xi zz}$, $\partial_{\xi\xi z}$, $\partial_{\xi\eta\eta}$, $\partial_{z\xi\xi}$, $\partial_{\xi\eta z}$, or $\partial_{z\eta\eta}$ may have relevance to the microscopic structures, such as surface steps of the crystal.[9,10,17]

B. (110) and (111) faces

The intensity (bulk contribution) of SHG from the (110) face is about an order of magnitude larger than that from the (001) face. The rotation-angle dependence of this bulk contribution has been studied experimentally by Bloembergen,[2] and was found to be in good agreement with a model in which only the bulk contribution is present. For the (110) face, only one reconstruction form, (1×1), is known. The "reactivity" of this surface, being a natural cleavage surface, is believed to be low, probably because of the surface relaxation toward a local structure represented by the sp^2 hybridized Ga orbital and the sp^3 hybridized As orbital with a lone pair extruding from the (110) plane with an angle.[18] Therefore, not much work has been done on the SHG change due to a surface modification.

Figures 7 and 8 show the bulk SHG on a singular and a vicinal surface of (110) tilted by 0.1 rad (5.7°) toward [100], respectively. On the (110) surface, the effect of vicinality is much smaller than that on the (001) face.

For (111) faces, much less has been studied by surface second-harmonic generation. We show, for future reference, in Figs. 9 and 10, the bulk-only contributions for a singular surface and a vicinal surface tilted toward [100] by 0.1 radian, respectively. We note that for the $S_{in}-S_{out}$ and $P_{in}-S_{out}$ cases a full sixfold symmetry is obtained on the singular surface, while a threefold symmetry is observed for the $P_{in}-P_{out}$ and $S_{in}-P_{out}$ cases. Also for the (111) faces, the effect of vicinality is smaller than that on the (001) face.[9,10]

IV. CONCLUSIONS

We have shown that the symmetry in the rotation-angle dependence of surface second-harmonic generation gives a clue for determining which surface tensor elements are involved, although, in general, a unique determination is not possible. Another advantage of observing the rotation-angle dependence is that any small surface contribution is magnified by interference with the strong bulk component. We have also shown that a small offset of the crystal cut (vicinal surfaces) causes a significant anisotropy for the (001) face.

ACKNOWLEDGMENT

The authors are grateful to Yoshifumi Katayama and Masao Tamura for a critical reading of the manuscript.

[1]See, for example, T. F. Heinz, in *Nonlinear Surface Electromagnetic Phenomena,* edited by H. Z. Ponath and G. I. Stegeman (Elsevier, Amsterdam, 1991), Chap. 5.

[2]N. Bloembergen, *Nonlinear Optics* (Benjamin, New York, 1965).

[3]R. K. Chang and N. Bloembergen, Phys. Rev. **144**, 775 (1966).

[4]T. Stehlin, M. Feller, P. Guyot-Sionnest, and Y. R. Shen, Opt. Lett. **13**, 389 (1988).

[5]J. E. Sipe, D. J. Moss, and H. M. van Driel, Phys. Rev. B **35**, 1129 (1987); J. E. Sipe, J. Opt. Soc. Am. B **4**, 481 (1987).

[6]C. Yamada and T. Kimura, Phys. Rev. Lett. **70**, 2344 (1993).

[7]V. B. Beretsetsky, E. M. Lifshits, and L. P. Pitaevsky, *Relativistic Quantum Theory* (Nauka, Moscow, 1968), Vol. 1.

[8]P. N. Butcher and D. Cotter, *The Elements of Nonlinear Optics* (Cambridge University, Cambridge, England, 1990).

[9]C. W. von Hasselt, M. A. Verheijen, and Th. Rasing, Phys. Rev. B **42**, 9263 (1990).

[10]M. A. Verheijen, C. W. von Haaselt, and Th. Rasing, Surf. Sci. **251/252**, 467 (1991).

[11]P. Guyott-Sionnest, W. Chen, and Y. R. Shen, Phys. Rev. B **33**, 8254 (1986).

[12]B. Koopmans, F. van der Woude, and G. A. Sawatzky, Phys. Rev. B **46**, 12 780 (1992).

[13]G. Lüpke, G. Marowsky, R. Steinhoff, A. Friedrich, B. Pettinger, and D. M. Kolb, Phys. Rev. B **41**, 6913 (1990).

[14]S. Ohkouchi and I. Tanaka, Jpn. J. Appl. Phys. **30**, L1826 (1991).

[15]I. Tanaka and S. Ohkouchi, Jpn. J. Appl. Phys. **32**, 2152 (1993).

[16]A full mathematical expression of the SH intensity for the $P_{in}-P_{out}$ case is given below:

$$I(P_{in}-P_{out}) \propto \left| \left\{ \frac{\cos^2\theta \sin\theta}{(N^2\cos\theta+NF_c)(n\cos\theta+nf_c)} \right\} \left\{ \frac{\cos^2\theta \sin\theta}{(N^2\cos\theta+NF_c)(n\cos\theta+nf_c)} \right\} \times \left\{ \left[\frac{32\pi NF_c nf_c - 16\pi}{(NF_c+nf_c)} \right] \sin 2\varphi + 8\pi \partial_{\xi\xi z} NF_c nf_c (1-\sin 2\varphi) \right\} \right|^2 .$$

[17]S. Janz, K. Pedersen, and H. M. van Driel, Phys. Rev. **44**, 3943 (1991).
[18]W. Ranke and J. Jacobi, Prog. Surf. Sci. **10**, 1 (1981).
[19]S. R. Armstrong, R. D. Hoare, M. E. Pemble, I. M. Povey, A. Stafford, and A. G. Taylor, J. Cryst. Growth **120**, 94 (1992).
[20]C. Yamada and T. Kimura, J. Cryst. Growth **130**, 321 (1993).
[21]S. R. Armstrong, R. D. Hoare, M. E. Pemble, I. M. Povey, A. Stafford, and A. G. Taylor, J. Cryst. Growth **130**, 323 (1993).